LBL--29733

DE91 005208

Very Hot Nuclear Systems and Their Binary and Multifragment Decay

L.G. Moretto, Y. Blumenfeld*, D. Delis, and G.J. Wozniak

Nuclear Science Division, Lawrence Berkeley Laboratory
University of California, Berkeley, California 94720, USA

October 1990

This work was supported by the Director, Office of Energy Research, Division of Nuclear Physics of the Office of High Energy and Nuclear Physics of the U.S. Department of Energy under Contract DE-AC03-76SF00098

VERY HOT NUCLEAR SYSTEMS AND THEIR BINARY AND MULTIFRAGMENT DECAY

L.G. MORETTO, Y. BLUMENFELD*, D. DELIS, and G.J. WOZNIAK

Nuclear Science Division, Lawrence Berkeley Laboratory,
1 Cyclotron Road, Berkeley, CA 94720

Abstract: Compound emission of complex fragments in the reaction $^{63}Cu + ^{12}C$ is used to determine the associated ridge-line potential. Compound binary emission of complex fragments at higher energies is illustrated for a variety of reactions. Complex fragment emission from 18, 26, 31, 35, 45 and 55 MeV/N $^{139}La/^{129}Xe + ^{12}C$, ^{27}Al, ^{40}Ca, ^{51}V, ^{nat}Cu and ^{139}La reactions has been studied. Multifragment events from these reactions were assigned to sources characterized by their energy and mass through the incomplete-fusion-model kinematics. Excitation functions for the various multifragment channels appear to be nearly independent of the system and bombarding energy. Preliminary comparisons of the data with sequential-statistical-decay calculations are discussed.

1. INTRODUCTION

How hot can a nucleus be? A critical temperature above which the liquid and the vapor phases of the nuclear fluid lose their identity has been postulated on the basis of the standard theory of classical fluids[1]. Nuclei, however, are at best tiny drops of this fluid, and they are affected very much by long range forces, like the Coulomb force. This may change the picture drastically, both regarding the exact value of the critical temperatures and regarding the existence or not of a relatively sharp second-order transition.

At present, it is not clear how this loss of stability should manifest itself, especially in view of the fact that nucleonic and complex fragment emission does already occur well below the expected onset of this instability. Extended, highly thermalized sources have been demonstrated in many heavy ion collisions. Neutron multiplicities and temperature determinations lead to the confirmation of excitation energies as high as 4-5 MeV/N[1,2]. Long-lived intermediate systems have been characterized in terms of their mass, charge, excitation energy and, to a more limited extent, angular momentum from their binary decay into complex fragments. In many instances it turns out that this complex fragment emission follows the statistical branching ratios expected for compound nucleus decay. This makes these intermediate systems honest-to-goodness compound nuclei, with excitation energies quite near

the expected maximum[1,3]. Furthermore, the rare compound nucleus emission of complex fragments at low energy[4,5] is consistent with the abundant emission observed at higher energies[1].

In this paper we are going to consider two aspects of complex fragment emission. The first deals with the demonstration that a good fraction of complex fragments arises from binary compound nucleus decay. The second considers the simultaneous emission of several fragments observed in the reactions $^{139}La + ^{12}C$, ^{27}Al, ^{40}Ca, ^{51}V, ^{nat}Cu and ^{139}La at various energies and tries to show the statistical nature of the process.

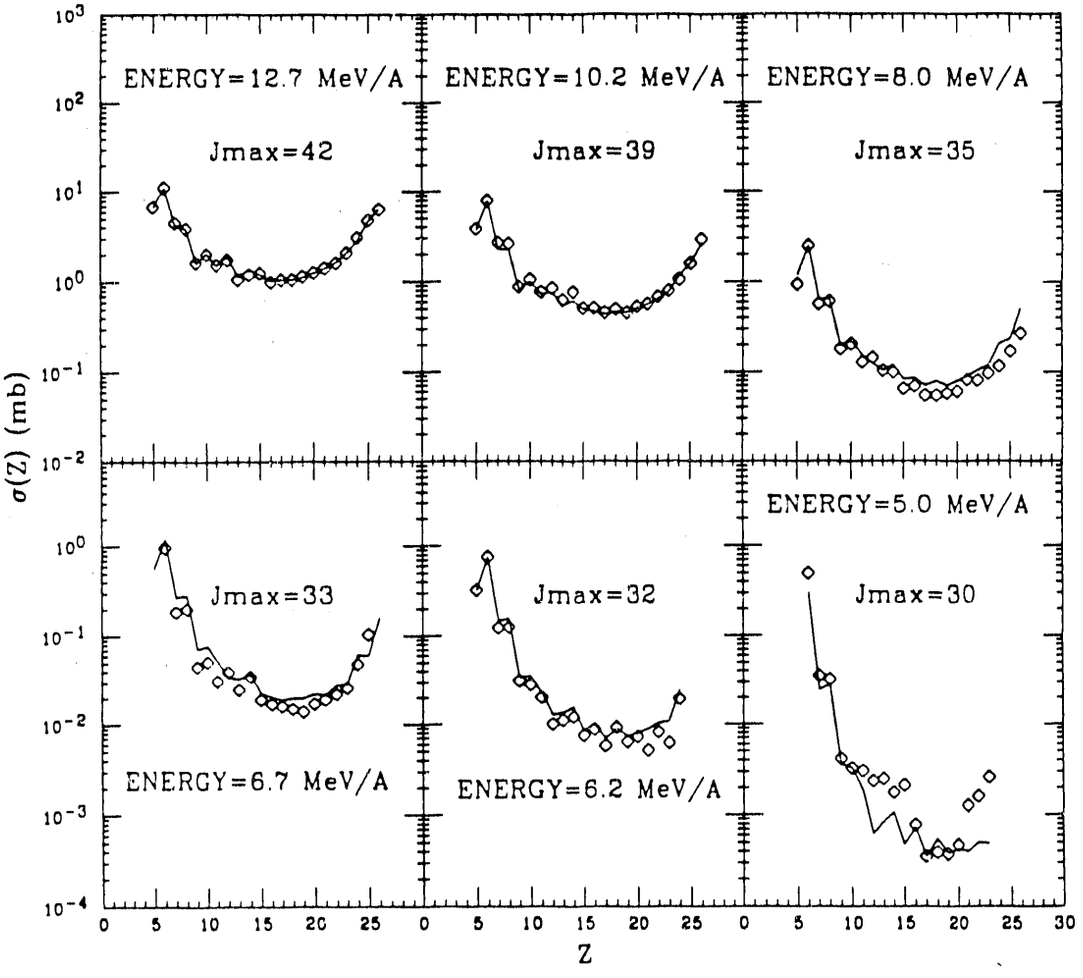

Figure 1

Cross sections as a function of atomic number for the reaction $^{63}Cu + ^{12}C$ at the indicated energies. The diamonds represent the experimental data, while the solid lines are the compound nucleus fits[6].

2. Compound Nucleus Decay and Complex Fragment Emission

The best way to prove the compound nucleus origin of complex fragments is to measure their excitation functions very near threshold. This has been done for a limited range of light

complex fragments for the reaction $^{3}He + ^{nat}Ag$[5]. The measured excitation functions were indeed characteristic of compound nucleus emission, and the extracted conditional barriers for each of the fragments were in excellent agreement with the predictions of the finite range model.

A very recent study[6] of the excitation functions for the entire range of fragments emitted in the reaction $^{63}Cu + ^{12}C$ proves the compound nucleus hypothesis throughout the entire mass asymmetry range, as shown by the charge distributions and the corresponding compound nucleus fits in Fig. 1. The extracted conditional barriers, together with the ratios of level density parameters at the saddle and for the residual nucleus after neutron decay, are shown in Fig. 2. Again the agreement of the extracted barriers with the finite range model predictions is excellent, while the liquid drop model predictions overestimate the experimental values by ~14 MeV.

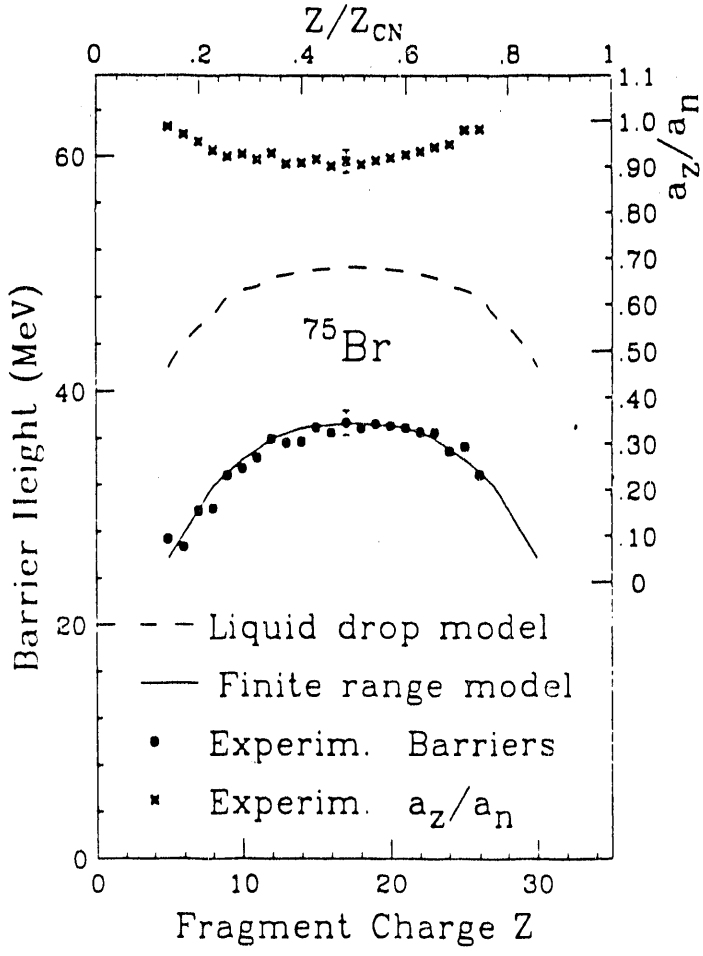

Figure 2

Emission barriers and a_z/a_n ratios as a function of atomic number extracted from the fits shown in Fig. 1.

A number of reactions have been studied at progressively higher incident energies. Many of these reactions have been studied in reverse kinematics to facilitate the detection of most of the fragments over a large center-of-mass angular range[1,3,7,8].

Absolute cross sections as a function of Z value for some of these reactions are shown in Figs. 3 & 4. At first glance one can observe a qualitative difference between the charge distributions from the ^{93}Nb-induced[3] and the ^{139}La-induced[8] reactions. The former distributions portray a broad minimum at symmetry, whereas the latter show a broad central fission-like peak that is absent in the former distributions. This difference can be traced to the fact that the former systems are below or near the Businaro-Gallone point, while the latter systems are well above it.

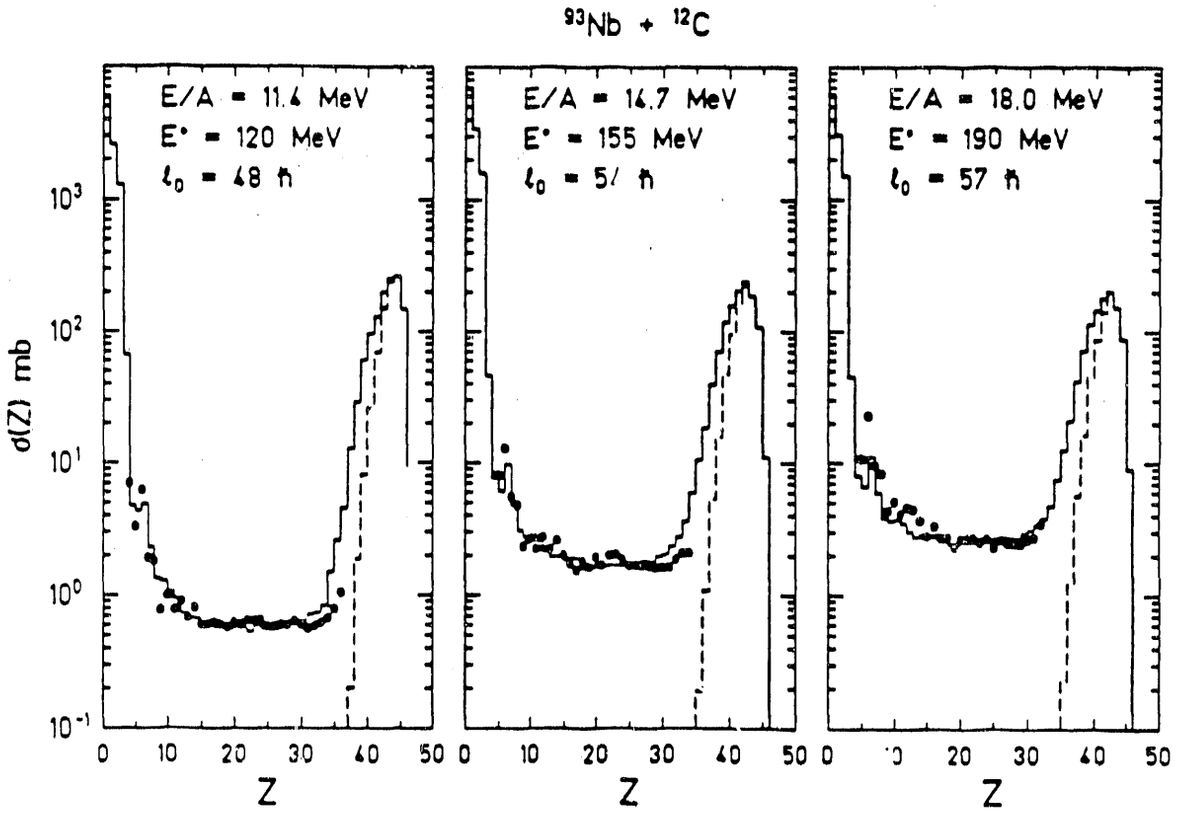

Figure 3

Angle-integrated cross sections (solid circles) plotted as a function of the fragment Z-value for the ^{93}Nb + ^{12}C reaction at 11.4, 14.7 and 18.0 MeV/N. The histograms represent calculations with the statistical code GEMINI[3]. The dashed curves indicate the cross sections of light particles ($Z \leq 2$). Note the value of the excitation energy (E^*) corresponding to complete fusion and the value of J_{max} assumed to fit the data[3].

In general, for a given system, the cross sections associated with the charge distributions increase in magnitude rapidly at low energies, and very slowly at high energy, in a manner consistent with compound nucleus predictions. The most important information associated with these cross sections is their absolute value and their energy dependence. Through them, the competition of complex fragment emission with the major decay channels, like n, p, and α

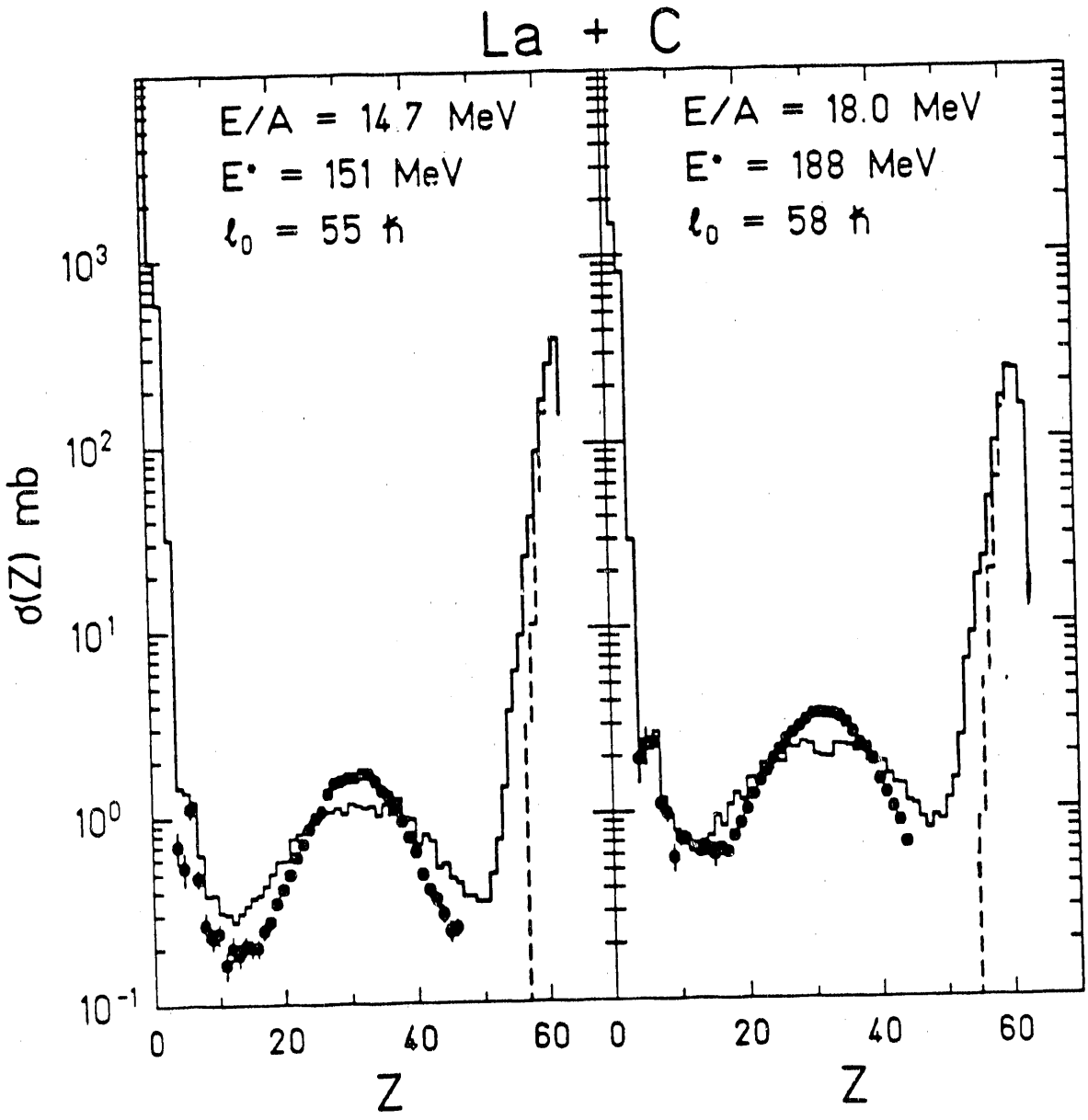

Figure 4

Same as Figure 3 for the 14 & 18 MeV/N $^{139}La + ^{12}C$ reactions.

decay is manifested. This is why we attribute a great deal of significance to the ability to fit such data. Examples of these fits are shown in Figs. 3 & 4. The calculations were performed with the evaporation code GEMINI[3] extended to incorporate complex fragment emission. Angular-momentum-dependent finite-range barriers were used. All the fragments produced were allowed to decay in turn both by light particle emission or by complex fragment emission. In this way higher chance emission, as well as sequential binary emission, was accounted for[3,8]. The cross section was integrated over ℓ waves up to a maximum value that provided the best fit to the experimental charge distributions. In the case of the $^{93}Nb + ^{9}Be$ &

^{12}C, as well ^{139}La + ^{12}C for bombarding energies up to 18 MeV/N, the quality of the fits is exceptionally good and the fitted values of ℓ_{max} correspond very closely to those predicted by the Bass model or by the extra-push model[3].

3. The Incomplete Fusion Model and the Source Velocity Analysis

In its simplest version, the geometric model of incomplete fusion implies the fusion between the heavier partner with the geometrically occluded portion of the lighter partner. The resulting fusion product can be assigned a preevaporation mass and an excitation energy just from the determination of its velocity. In particular, this velocity can be determined from the binary, ternary, etc. coincidences of the decay products. If a given combination of target and projectile can give rise to incomplete fusion over a broad range of impact parameters, the resulting fusion products will have a correspondingly broad range of excitation energies. In this way, excitation functions for the various decay modes of the fusion products can be obtained at a single bombarding energy.

The process of incomplete fusion depends not only upon the bombarding energy but, and perhaps just as strongly, upon the entrance channel mass asymmetry.

In Fig. (5) binary event contour plots in the source velocity - Z_{Total} plane are shown for a series of targets and bombarding energies in La-induced reactions. In the case of light targets (C, Al), one observes essentially a single source, characterized by a well defined Z_{Total} and bombarding energy. For the heavier targets (Ti, Cu/Ni), however, a broad distribution of sources is identifiable. Perhaps, the most impressive distributions are those at the lowest bombarding energy, where the source velocities are seen to decrease dramatically with an increase in total charge. This correlation, which can be taken as a rather vivid description of the incomplete fusion model, tends to disappear at higher bombarding energies. The reason is not associated with a failure of the model. Rather, at higher bombarding energies, the excitation energy brought in by the fusing portion of the target becomes so high that it is accompanied by an ever increasing secondary evaporation of charged particles. Consequently, the correlation between source velocity and total charge is lost.

4. Multifragment Decay of Hot Systems

Multifragment decay is a process not well characterized at present nor well understood. On the one hand, it is not clear whether it is a dynamical or statistical process. On the other it is not clear whether the fragments are emitted simultaneously or sequentially. In order to shed light on these problems we have studied the multifragment emission in the reaction ^{139}La + ^{12}C, ^{27}Al, ^{40}Ca, & ^{51}V at 35 and 40 MeV/N[9]. The beam energies were chosen in order to produce systems with high excitation energies while remaining in a domain where the incomplete fusion model should retain its validity.

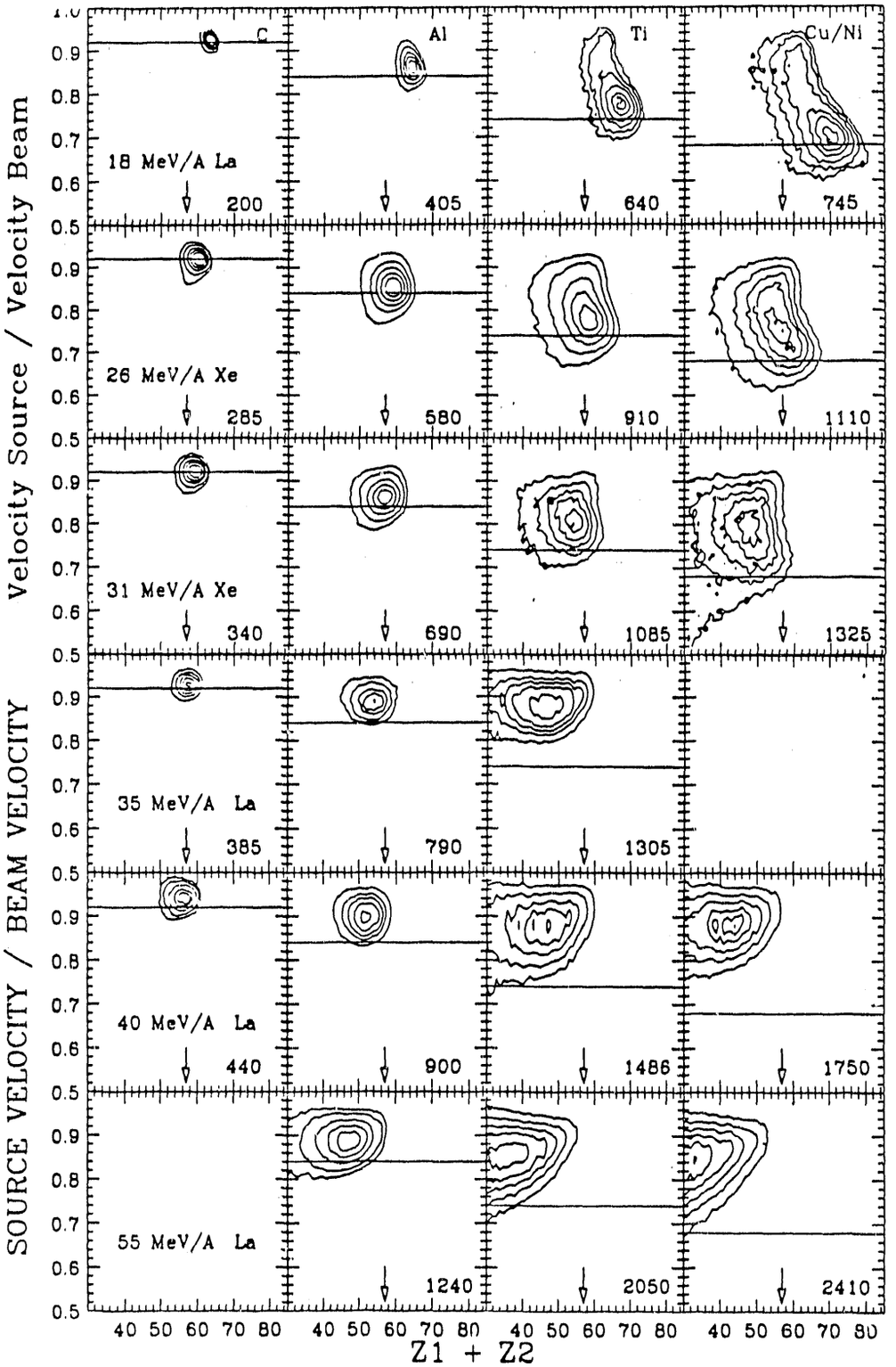

Figure 5

Contour plots in the $v_{\|}$ - Z_{1+2} plane for the reactions $^{139}La/^{129}Xe + ^{27}Al$, $^{48}Ti/^{51}V$, $^{64}Ni/^{nat}Cu$ at 18, 26, 31, 35, 40, 55 MeV/N. The horizontal lines, vertical arrows and the number in the lower right hand corner indicate the complete fusion velocity, projectile charge and the available energy in the c.m., respectively.

4.1. Summed Charge Distributions

Figure 6 (a-d) presents the distributions of the sum of the measured charges for 2-fold events at E_{lab} = 35 MeV/N. (An n-fold event is defined as an event where n fragments of charge Z>4 were detected.) For the ^{12}C target a narrow peak is observed. This peak broadens for heavier targets, reflecting the wider range of excitation energies resulting from the larger range of mass transfers, which gives rise to increasing amounts of light particle evaporation. With increasing target mass, the tailing to low Z values increases. This tail is due to 3- or 4-body events where only two bodies were detected, and shows the increasing importance of multibody reactions for the heavier targets. The same distributions for 3- and 4-fold events (Figs. 7b,c for $^{139}La + ^{40}Ca$) exhibit a peak at approximately the same total charge as the 2-fold events, but with a reduced low Z continuum, showing that most of these multi-fold events

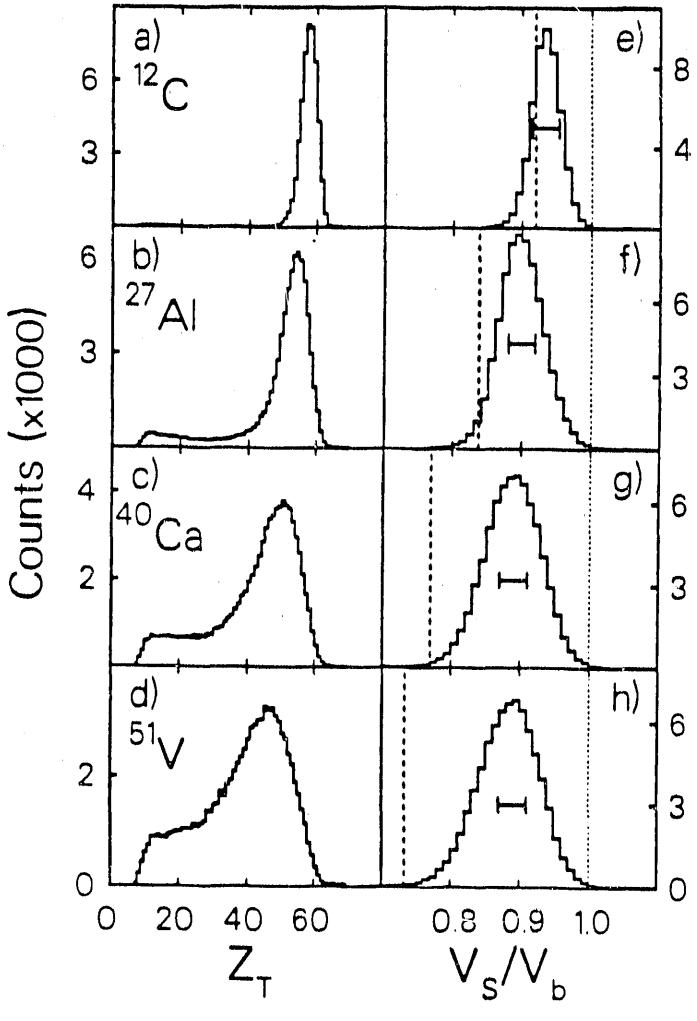

Figure 6

a-d) Distributions of the sum of the measured charges for 2-fold events for the 35 MeV/N $^{139}La + ^{12}C$, ^{27}Al, ^{40}Ca and ^{51}V reactions. e-h) Distributions of source velocities expressed as the ratio of the source to beam velocity for the same reactions. The dotted line indicates the beam velocity, and the dashed lines the source velocities expected for complete fusion. The horizontal bars indicate the expected broadening of the source velocity distribution due to light particle evaporation for the mean excitation energy.

are essentially complete.

4.2. Source Velocities

The following analysis is restricted to events whose total measured charge is at least 30, in order to insure a reasonable representation of the kinematical skeleton of the reaction. If the fragments originate from the decay of a single source, then its velocity is determined by $\mathbf{V_s} = \{\Sigma_i m_i \mathbf{V_i}\}/\Sigma_i m_i$. In the incomplete fusion picture[9], the excitation energy E^* is approximately related to the parallel source velocity V_s by $E^* = E^b(1-V_s/V_b)$,where E_b is the bombarding energy and V_b the beam velocity. Although this formula does not take into account preequilibrium emission, it remains correct if the preequilibrium particles retain on average the target or projectile velocity. Also, the recoil of the target-like remnant due to the shearing-off of the fusing part is neglected, but calculations[10] show that, by including recoil effects, the excitation energies change by less than 20 MeV, which is much less than the experimental uncertainty.

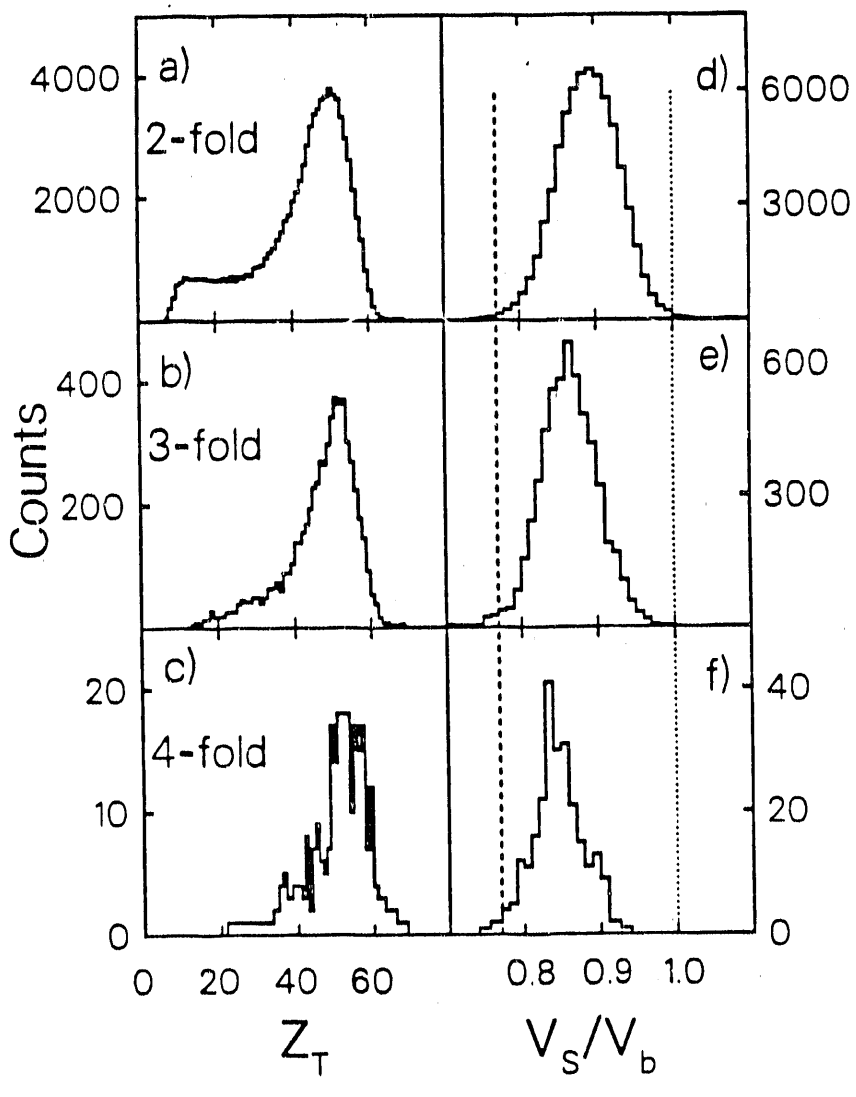

Figure 7

Same as Fig. 6 for 2-, 3- and 4-fold events from the $^{139}La + ^{40}Ca$ reaction at E_{lab} = 35 MeV/N.

Source velocity distributions for the ^{12}C, ^{27}Al, ^{40}Ca, and ^{51}V targets are presented in Fig.6 (e-h) for the 35 MeV/N bombarding energy. The peak of the distribution shifts downwards with increasing target mass showing that, on average, more mass is picked up from the heavier targets. The peak also broadens considerably when going from the ^{12}C to ^{51}V target. Part of this width is due to the actual range of source velocities, arising presumably from different impact parameters, and part to the perturbation introduced by light particle evaporation prior and subsequent to heavy fragment emission. This "noise" has been estimated with the statistical decay code GEMINI[3], filtered by the appropriate detector geometry, and is represented by the horizontal bars on Fig.6 (e-h). In the case of ^{12}C the width can be explained almost entirely by light particle evaporation, showing that, due to the interplay between the incomplete fusion mechanism and the complex fragment decay probability, a very limited range of excitation energies contributes to complex fragment emission. However, this is no longer the case for the heavier targets, where a large range of excitation energies is indeed observed.

When the events are separated according to the fragment multiplicity (see Fig.7 (d-f)), the requirement of a larger multiplicity of complex fragments selects out events with lower source velocities, i.e. higher excitation energies. For the ^{40}Ca target at E_{lab} = 35 MeV/N, the estimated most probable excitation energies are 530, 660, and 750 MeV for 2-, 3-, and 4-fold events, respectively. The same trend is observed for all targets. A similar result was recently observed in the ^{20}Ne+ ^{197}Au reaction at 60 MeV/N, but only for 2- and 3- body final states[11]. To check that this result is not due to some experimental artifact, we have generated with the statistical code GEMINI a set of binary and multibody events resulting from the decay of a nucleus at a given excitation energy. Assuming a fixed source velocity, the results were filtered by the detector acceptance, then the source velocity was reconstructed using the same analysis code as for the experimental data. In this simulation the mean source velocities were the same for different multiplicities, indicating that the experimental detection efficiency is not skewing the multibody results significantly.

4.3. Excitation Functions

Excitation functions for the multi-fold events have been determined by inferring the excitation energies from the source velocities. The cross section for multibody events at a given excitation energy depends on the probability of producing nuclei with this excitation energy via the incomplete fusion process. In order to remove this dependence, we have plotted the proportion of n-fold events with respect to the total number of coincidence events: $P(n) = N(n)/(N(2)+N(3)+N(4)+ ....)$,where N(n) is the number of n-fold events. Evaporation residues (1-body events) were not considered since in reverse kinematics they are confined to a very small angle around the beam direction where our detection efficiency is small. These excitation functions (Fig.8) have not been corrected for the detection efficiency. Such a

correction requires knowledge of the precise kinematical nature of the events, such as mass distributions and relative velocities of the fragments, and will not be attempted here. Nevertheless, several remarkable features can be noted.

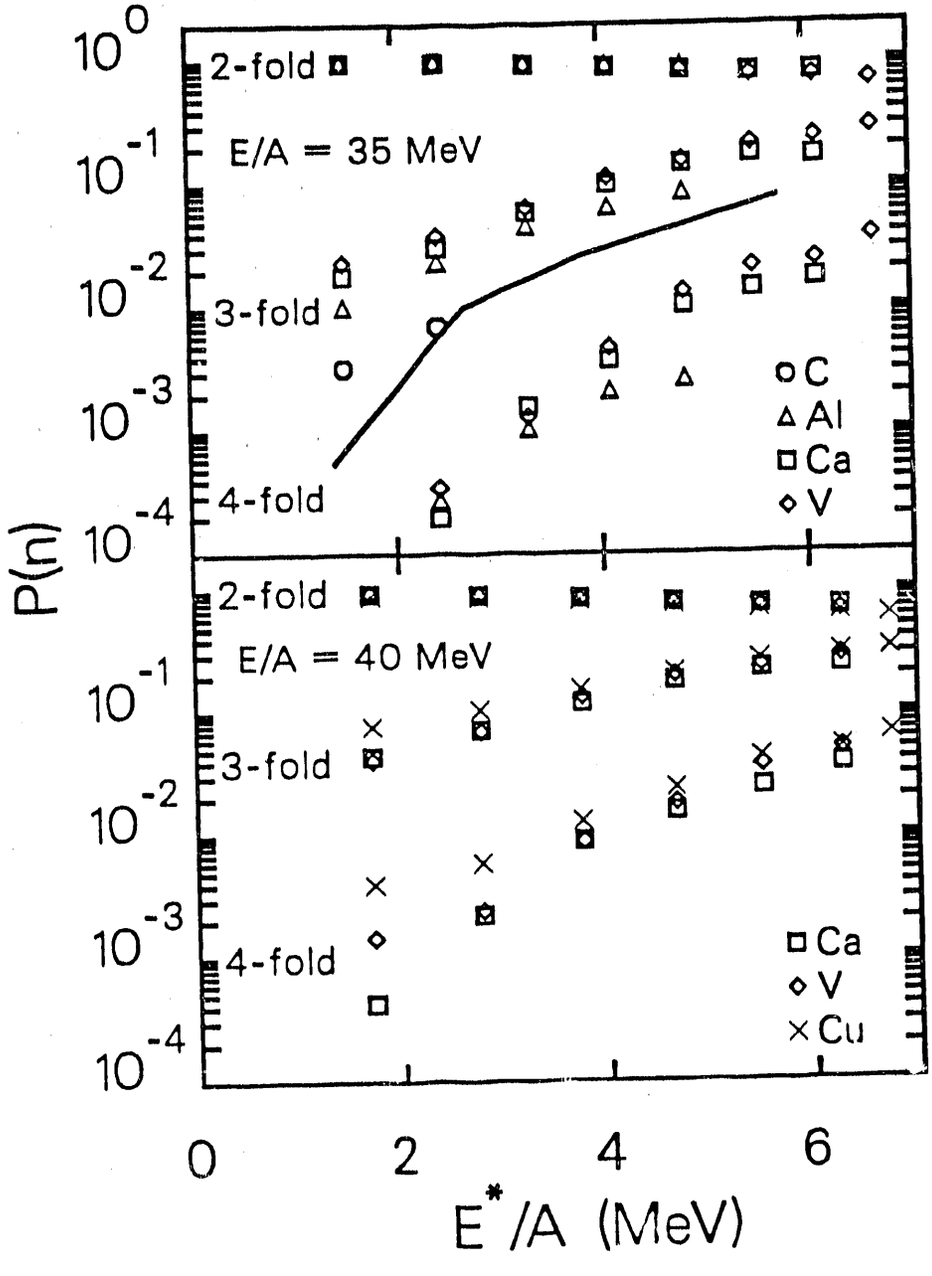

Figure 8

Proportion of 2-, 3-, and 4-fold events as a function of excitation energy per nucleon for the targets studied at E_{lab} = 35 MeV/N (top) and 40 MeV/N (bottom). The estimated masses of the hot nuclei vary from 145 at 2 MeV/N to 175 at 6 MeV/N. The solid line is the result of a statistical calculation with the code GEMINI for 3-fold events (see text).

First, the probabilities for 3- and 4-fold events increase substantially with the excitation energy of the source up to the highest energies observed (~1000 MeV or 6 MeV/N). Such behavior would be expected from any statistical model and is an *a posteriori* verification of the relation between source velocity and excitation energy over the entire source velocity range studied. This energy dependence also confirms that the width of the velocity distribution originates mostly in the incomplete fusion process, and is only partly due to sequential light particle decay.

Second, the relative proportions of multi-fold events for the three heaviest targets and the two bombarding energies are very similar, suggesting that the sources produced in these reactions depend mainly on how much mass is picked up by the projectile from the target, and relatively little on the actual nature of the target. This is precisely what constitutes the essence of the incomplete fusion model! A closer look at Fig.8 shows a slight decrease of the multi-fold probability for lighter targets, as well as for the lower bombarding energy for a given target. One possible contribution to these minor discrepancies is the effective broadening of the excitation energy bins due to light particle evaporation, which is particularly severe in the case of the lightest targets for which evaporation is a major contribution to the width of the source velocity distribution (Fig 6). In particular this could explain why the multi-fold probabilities for the ^{27}Al target at the highest excitation energies, which are in the tail of the source velocity distribution, fall significantly below those measured for ^{40}Ca and ^{51}V. Moreover, the transition state model of statistical decay[12] predicts a strong decrease of the complex fragment decay probability with decreasing angular momentum[13]. Thus, an additional source of the differences could be that the hot nuclei are formed in the various reactions with slightly different angular momenta.

Finally, the proportion of multi-fold events increases smoothly with excitation energy up to approximately 6 MeV/N. The statistical multifragmentation calculations of Bondorf et al.[14] predict a sudden rise in the multibody probability at ~3 MeV/N for a nucleus of mass 100. Gross et al.[15] predict a similar transition towards nuclear cracking at an excitation energy of ~5 MeV/N for a ^{131}Xe nucleus. Experimentally, we see no evidence for such phase transitions, and the data suggest that the decay of the hot nuclei under study (A~160) is governed by the same mechanism up to an excitation energy approaching the total binding energy of these nuclei.

More recent studies performed at higher bombarding energies and with a broad range of targets confirm the features illustrated so far. In Fig. 9 we observe again that the excitation functions seem to be remarkably independent of both bombarding energy and target. Most impressive are the highest excitation energies that are inferred for these systems. They extend up to 8 MeV per nucleon; thus if our interpretation is correct, we are dealing with nuclei whose excitation energy equals the total binding energy!

In order to investigate if this mechanism could be the sequential statistical decay of an equilibrated compound nucleus, calculations were performed using the code GEMINI. Several excitations energies between 200 and 1000 MeV were studied. The initial mass and angular momentum of the compound nucleus corresponding to each excitation energy was calculated with the incomplete fusion model of Moretto and Bowman[10]. Between the two extreme excitation energies considered, the masses range from 145 to 175 and the angular momenta from 40 to 100 ħ. For each event, the code outputs the charge, mass and velocity vector of each fragment. Assuming the source velocity given by the incomplete fusion calculation, the results were filtered by the detector acceptance, taking into account the beam spot size, and the angular divergence of the beam.

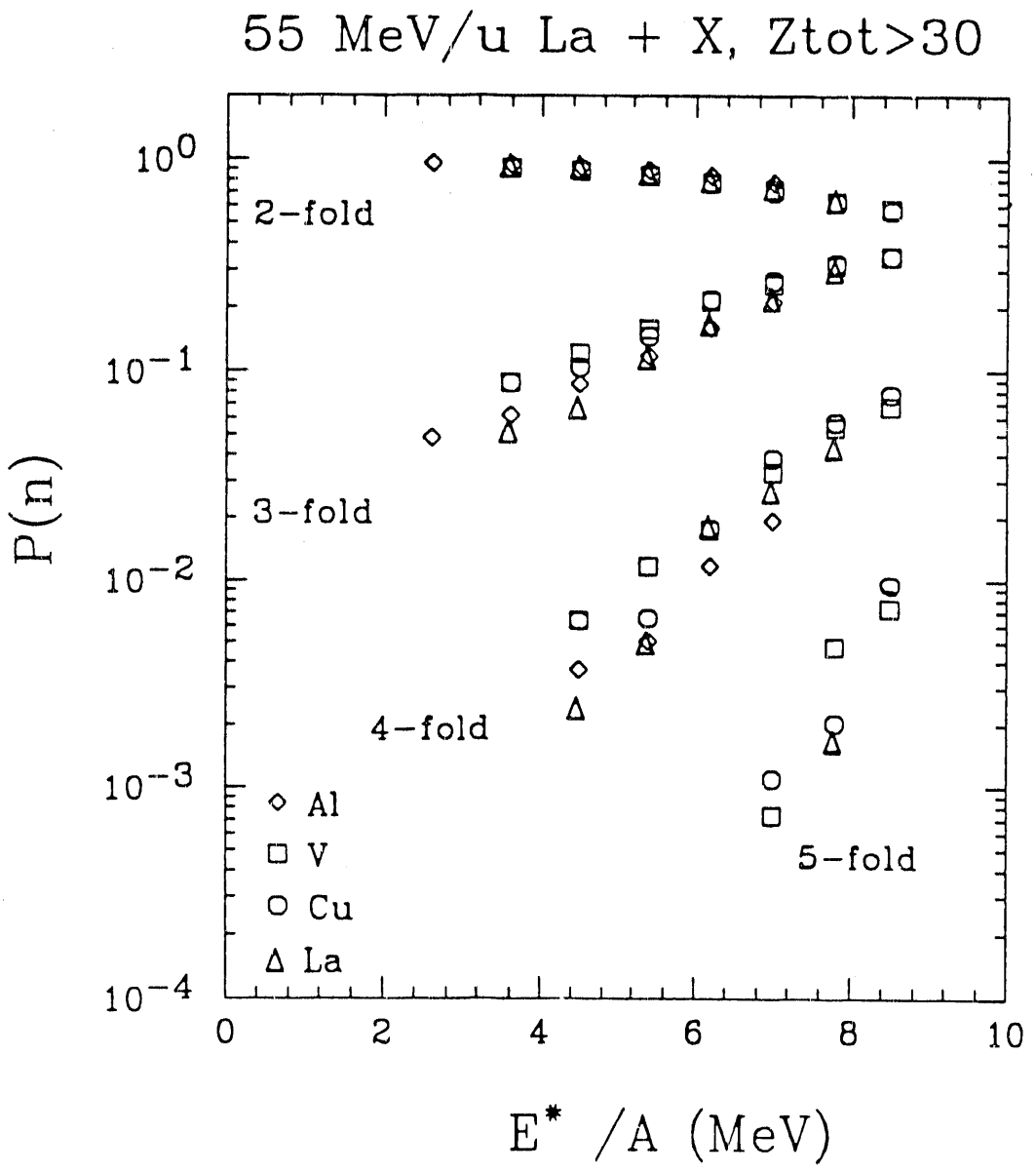

Figure 9
Same as in Figure 8 for the reactions $^{139}La + ^{27}Al$, ^{51}V, ^{nat}Cu, and ^{139}La at 55 MeV/N.

The results for 3-fold events is shown as a solid line in the top part of Fig. 8. The trend of the data is nicely reproduced, but the absolute proportion of 3-fold events is underestimated by about a factor of 2. Moreover the proportion of 4-fold events predicted by the calculation is almost a factor of 10 too low. As discussed before, this could be due to an imprecise estimate of the angular momentum in the incomplete fusion model. Another possibility would be the pre-equilibrium emission of at least one of the fragments. Such pre-equilibrium emission of intermediate mass fragments has already been observed[16], and a hint for such a behavior in the present data is given by the inclusive angular distributions of the light fragments which are strongly backward peaked in the source frame.

4. CONCLUSIONS

In this talk we have presented evidence for binary compound emission of complex fragments at low and moderate excitation energies. Furthermore, the source velocity technique[7] was extended to multibody events and employed in conjunction with the incomplete fusion model to estimate the excitation energy on an event-by-event basis. This, in turn, has allowed us to present for the first time excitation functions for multifragment events. These excitation functions are largely independent of target-projectile combination and of bombarding energy, lending support to the incomplete fusion picture and to the idea of an intermediate system whose decay properties depend only on its excitation energy and angular momentum. Up to an excitation energy of 1200 MeV (~8 MeV/N), no evidence for a phase transition towards nuclear cracking was found.

*On leave from Institut de Physique Nuclèaire, Orsay, France

ACKNOWLEDGEMENT

This work was supported by the Director, Office of Energy Research, Office of High Energy and Nuclear Physics, Division of Nuclear Physics, of the U.S. Department of Energy under Contract No. DE-AC03-76SF00098.

REFERENCES

1) Moretto L. G. and Wozniak G. J. , 1988 *Prog. in Part. & Nucl. Phys.* **21** 401 and references therein.
2) Guerreau D.,1989 *Int'l. School on Nuclear Physics : Nuclear matter and Heavy Ion Collisions*, Les Houches, France, Preprint Ganil P89-07.
3) Charity R.J. et al., 1988 *Nucl. Phys.* **A483** 371.
4) Sobotka L. G. et al., 1983 *Phys. Rev. Lett.* **51** 2187.
5) McMahan M. A. et al., 1985 *Phys. Rev. Lett.*, **54** 1995.

6) Delis D. N. et al., 1990 Lawrence Berkeley preprint No. LBL-28940, submitted to *Phys. Rev. Lett.*
7) Colonna N. et al., 1989 *Phys. Rev. Lett.* **62** 1833.
8) Charity R. J. et al., 1990 *Nucl. Phys.* **A511** 59.
9) Blumenfeld Y. et al., Lawrence Berkeley Laboratory preprint No. LBL-28472, submitted to *Phys. Rev. Lett.*
10) Moretto L.G. and Bowman D.R. 1986 in *Proc. of the XXIV Int'l. Winter Meeting on Nuclear Physics, Bormio, Italy*, edited by I.Iori [Ric. Sci. ed. Educazione Permanente, Suppl.49, (1986) 126].
11) Bougault R. et al., 1989 *Phys. Lett.* **B232** 291.
12) Moretto L.G., 1975 *Nucl. Phys.* **A247** 211.
13) Charity R. J. et al., 1988 Nucl. Phys. **A476** 516.
14) Bondorf J., Donangelo R., Mishustin I. N., and Schulz H., 1985 *Nucl. Phys.* **A44** 460.
15) Gross D.H.E., Yu-ming Zheng and Massman H., 1987 *Phys. Lett.* **B200** 397.
16) Yennello S. J. et al., 1990 *Phys. Rev.* **C41** 79.

END

DATE FILMED

01 / 18 / 91